Effect of Different Solvents on Performance Polymer: Fullerene: Gold Nanoparticles Organic Solar Cell

Dr.Abdullah Abbas Hussein
Material Science Department, Polymer Research Centre, University of Basrah / Basrah.
Email:amanar_2005@yahoo.com
Dr.Waleed Ali. Hussain
Physics Department, college of education, University of Basrah
Dr.Hussein Falih Hussein
Physics Department, college of education, University of Basrah

ABSTRACT

   Gold nanoparticles (AuNPs) deposited at the interface of the intermediate layer [poly (3,4ethylenedioxythiophene):poly(styrenesulfonate) (PEDOT:PSS)] and poly(3-hexylthiophene):[6,6]-phenylC61-butyricacidmethylester (P3HT:PCBM) active layer were found to significantly increase organic solar cell performance. Organic solar cell devices with different solvents, such as the chlorobenzene (CB), dichlorobenzene (DCB), chloroform (CF), and co-solvent Chlorobenzene: Dichlorobenzene (CB:DCB), Chlorobenzene:Chloroform (CB:CF), and Dichlorobenzene:Chloroform (DCB:CF) were fabricated. The photo-physical properties of these devices with different solvents are investigated. It can be found that, absorption spectrum of the blend becomes broad with different solvents, which is highly desirable for an organic solar cell devices. Film morphology is evaluated by Atomic Force Microscopy (AFM). XRD patterns and External Quantum Efficiency (EQE) measurements are also performed for the devices. The efficiency enhancement for the device with (CB:CF) is more significant than for other solvents. With different solvents, the solar cells upon (CB:CF) give Power Conversion Efficiency (PCE) of 3.6%, in contrast to 3.2% for (CB), 2.06% for (DCB), 3% for (CF), 2.55% for (CB:DCB), and 2.9% (DCB:CF) devices.
Keywords: P3HT:PCBM, Organic Solar Cell, Solvents, Gold nanoparticle.

<div dir="rtl">

تأثير اضافة مذيبات متنوعة على اداء الخلية الشمسية العضوية (بوليمر: فوليرين:جزئيات الذهب النانوية)

الخلاصة

   في هذا البحث تم تحضير الخلية الشمسية العضوية (PEDOT:PSS:AuNPs/P3HT: PCBM)، حيث تم دراسة اضافة مذيبات مختلفة مثل الكلوروبنزين (CB)، والداياكلوربنزين (DCB)،والكلوروفورم(CF)،والكلوروبنزين:الداياكلوربنزين(CB:DCB)، والكلوروبنزين: الكلوروفورم (CB:CF)، والدايا كلوربنزين:الكلوروفورم (DCB: CF) الى الطبقة الفعالة (:P3HT PCBM) في الخلية الشمسية، ومن ثم دراسة الخصائص الفيزيائية لها. حيث لوحظ من خلال هذه الدراسة حدوث توسع في طيف الامتصاص لعدد من المذيبات وهو امر مرغوب للحصول على كفاءة

</div>

خلية شمسية افضل. تم كذلك دراسة طبيعة السطح لكل الخلايا المحضرة من خلال استخدام جهاز
مجهر القوة الذرية (AFM) وانماط حيود الاشعة السينية (XRD) وكفاءة الكم الخارجية (EQE).
لوحظ من خلال قياس كفاءة الخلية الشمسية بان المذيب (CB:CF) يعطي افضل اداء من باقي
المذيبات الاخرى. ان قيم الكفاءة المستحصلة لكل الاجهزة المحضرة هي ,(3.6%= CB:CF)
.(CB=3.2%), (DCB=2.06%), (CF=3%), (CB:DCB=2.55%), (DCB:CF=2.9%)

INTRODUCTION

Converting solar energy into electrical energy is becoming significant due to the crisis in conventional energy sources nowadays. There are different natural resources available to generate energy. Converting solar energy into electrical energy is one of such exploitation of the natural sources. Inorganic solar cells are the best utilized for the last few decades in this direction. But, the drawbacks such as manufacturing high costs and difficult fabrication process made researchers to look into easily processable nature and low cost polymer materials. Much work has been done for almost last one decade on polymer solar cells, but the lower power conversion efficiency (PCE) limits their commercial usage [1–3]. After introduction of bulk heterojunction concept, the PCE of polymer solar cells is nearing to 5% [4].

But, these values are not sufficient to meet realistic specifications for commercialization.

The formation of bulk-heterojunction phase allows for bulk separation of photoinduced excitons and high-mobility removal of electron through the nanophase. Poly(3- hexylthiophene) (P3HT) has been the mostly used p-type material [3, 4] in polymer solar cells along with a fullerene derivative, [6,6]-phenyl C61- butyric acid methyl ester (PCBM) as an electron acceptor. Since hole is typically the high-mobility carrier in regioregular P3HT [5], the enhanced electron mobility was achieved by addition of electron acceptor. However, the difficulty in these systems arises when we account for the effects of morphological modifications in P3HT phase due to the introduction of nano-phase [6]. There are significant number of studies that investigate the effects of processing parameters on blended photoactive nano-phase [7]. Even, the regioregularity and molecular weight [8] of P3HT also affect the performance of P3HT:PCBM devices. The electric power extracted from a photovoltaic device depends on both the photocurrent and photovoltage of the diode under illumination of a given intensity. In order to increase the PCE of a photovoltaic device, the practicable approach is to increase the photocurrent as much as possible, since the solar cell is limited by the built-in potential and it is the difference between the highest occupied molecular orbital (HOMO) and lowest unoccupied molecular orbital (LUMO) of the electron donor and acceptor materials [9].

Different device geometries and interface morphologies are evaluated for the purposes of trapping more light, dissociating excitons more efficiently, transporting charges with fewer impediments in order to extract more photocurrent [10]. Indeed, the solvents used for the preparation of active layer have shown a strong impact on its morphology, which influences the generation of photocurrent in the devices [11]. Unfortunately, till to date no conclusive result was made for optimal processing of the nano phase.

Experiment

Photovoltaic Device Fabrication

Pre-patterned indium tin oxide (ITO)-coated glass slides (80 nm thick, 10Ω/sq sheet resistance). The ITO substrates were first cleaned with ultrasonic in acetone and isopropyl alcohol for 10 min, heat dried in an oven at 120 0C and finally treated by ozone–ultraviolet cleaner for 10 min. The gold nanoparticles AuNPs were added to linear polystyrene (PS) in order to inhibit the dewetting in the spun-cast films. The PS acts as an inert host to improve the film forming property of the AuNPs [10]. The AuNPs solution was prepared by mixing the AuNPs with the PS (1:4 w/w) into the toluene solvent. A film of poly(ethylene dioxythiophene) (PEDOT: PSS:AuNPs) was spin cast on top of the ITO substrates with a speed of 2000 r/min for 40 s to form the hole- transport layer, and was dried for 15 min at 140 ^{0}C. Afterwards, the mixed solutions consisting of P3HT (10 mg mL-1, Sigma-Aldrich) and PCBM (`10 mgmL-1, Sigma-Aldrich) in different solvents (CB), (DCB), (CF), (CB:DCB), (CB:CF), and (DCB:CF) in 1:1 weight ratio were spin cast in a nitrogen-filled glove-box, then spin coated at 800 rpm on the PEDOT:PSS film to form the active layer. The thickness of the active layer is ~150 nm and thickness of the PEDOT:PSS layer (30 nm) . Finally, a bilayer cathode consisting of 100 nm Al was thermal evaporated under high vacuum of ~ 2×10^{-5} torr with a rate of 0.2 nm/s onto the polymer layer as a cathode to create a device with an active area of 9 mm^{2} defined by a shadow mask on the active layer to form cells with an active area of 1 cm^{2}.

Device Characterization

The current density–voltage (J–V) characteristics of devices were measured with a computer-programmed Keithley 2400 Digital SourceMeter and the photocurrent was generated under AM 1.5 G irradiation of 100 mWcm^{-2}. P3HT:PCBM films were prepared by spin coating P3HT:PCBM solution on glass substrates for UV–vis absorption spectroscopy and atomic force microscopy (AFM).The UV–vis absorption spectra of the polymer films were taken with a Varian Cary 5000UV– VIS–NIR spectrometer and Raman spectroscopy using a Horiba Jobin Yvon HR800 micro-Raman spectrometer. The light intensity for the solar simulator was calibrated with a standard photovoltaic (PV) reference cell. The AFM images of the polymer films were acquired using a BRUKER NanoScope IV Multi-Mode Adapter AFM with the tapping mode. The film thickness was determined with aTencorP-10 Alpha-Stepprofiler. The PCE is described by $\eta = FF\times (V_{oc} \times J_{sc})/P_{light}$, where the FF is defined as $FF= (Imax \times Vmax)/(I_{sc}\times V_{oc})$ and the Plight is the power of incident light. The PCEs of the pristine and hybrid OSCs were estimated for AuNPs .

Results and discussion

Figure (1) shows the UV–vis absorption spectra of P3HT:PCBM film (the thicknesses of all films ~ 160 nm) bulk heterojunctions prepared from different solvents, such as the (CB), (DCB), (CF), solvents and the (CB:DCB), (CB:CF), and (DCB:CF) co-solvents. An interesting effect was observed, the P3HT:PCBM bulk heterojunctions prepared from the CB:CF co-solvent showed the maximum absorption intensity and shifting in the wavelength in the visible wavelength ranging from ~ 400 to 650 nm compared to the other samples. It is observed that the absorption intensity of the bulk heterojunction are affected by the solvent species, indicating that a large number of photons are absorbed in the bulk heterojunction

dissolved by the CB:CF co-solvent. It is expected that the high value of the light absorption intensity could lead to an improvement and increase in the generation rate of excitons.

This result can also be explained by a change in the stacking conformation of the polymer structure from high crystallinity to lower crystallinity, and a reduction of intraplane and interplane stacking, which causes a poor π–π^* transitions and lower absorbance [12]. The portion of the spectra in the wavelength range lower than 400 nm for all solvents corresponds to the absorption of PCBM [13]. Figure (2) shows the XRD results from bulk heterojunction of P3HT:PCBM prepared by spin coating from various solvents *(CB), (DCB), (CF), (CB:DCB), (CB:CF), and (DCB:CF)* with thermal annealing at 125 ^{O}C for 15 min, respectively. The XRD intensity values were obtained peaks at $2\theta \approx 5.4$ for all solvents, where the reflection of (d_{100} -spacing) plane correspond to as describe by the (JCPDS 44-0558) [14]. These values are corresponding to the inter-chain spacing in P3HT associated with the interdigitated alkyl chains and indicating the degree of crystallinity of P3HT [15]. When high boiling point solvents, DCB (boiling point = 178 ^{O}C) and CB (boiling point = 132 ^{O}C), instead of low bp solvent, CF (boiling point = 61 ^{O}C), were used for Bulk heterojunction, the increased intensities were observed in the peak at $2\theta \approx 5.4$. This indicating that the bulk heterojunctions prepared from DCB and CB have the higher ordered structure and more improved crystallinity than CF. In the higher
bp solvents, P3HT in the bulk heterojunction may have longer time to solidity due to the slow evaporation rate of solvents and the slow film growth rate may assist to form high degree of self-organized structure [16].

In the case of mixed solvents, P3HT undergoes competitive film growth rate during spin-casting from solvents with two different vapor pressure and solubility. The P3HT in the bulk heterojunction prepared from a mixed solvent CF:CB is obtained more improved crystallinity than mono solvent such as CF and CB. However, crystallinity of P3HT was not improved when the bulk heterojunction prepared from a mixed solvent CF:DCB because DCB and CF have too different vapor pressure to occur competitive growth rate. In addition, after thermal annealing, the crystallinity was improved in the bulk heterojunction prepared from low boiling point solvent, especially CF, which has the fast solvent evaporation and film growth rate during spin coating [16].

Figure (3) shows the Raman spectroscopy of PEDOT:PSS:AuNPs /P3HT:PCBM film prepared from different solvents, such as the (CB), (DCB), (CF), solvents and the (CB:DCB), (CB:CF), and (DCB:CF) co-solvents, deposited on a Al substrate, are shown in Figure (3). It was characterized by Raman spectroscopy in the range 200-2000 cm^{-1}. TheRaman spectroscopy of PEDOT:PSS:AuNPs/P3HT:PCBM films with different solvents (CB), (DCB), (CF), (CB:DCB), (CB:CF), and (DCB:CF) doesn't differ from P3HT:PCBM film due to no Raman features attributable to PEDOT:PSS:AuNPs film and absence effect the different solvents on the PEDOT:PSS: AuNPs/P3HT:PCBM films. Therefore, The main in-plane ring skeleton modes are similar behaviour in P3HT, P3HT/PCBM, and P3HT:PCBM films previous, as below: at 1452 – 1468 cm^{-1} (symmetric C=C stretching mode) and at 1381-1391 cm^{-1} (C-C intra-ring stretching mode), the inter-ring C-C stretching mode at 1200-1210 cm^{-1}, the C-H bending mode with the C-C inter-ring stretch mode at 1180-1200 cm^{-1}, and the C-S-C deformation mode at 720-740 cm^{-1}.Similar results were also observed by pure P3HT with CB solvent only [17]. The microstructure of

the PEDOT:PSS:AuNPS/P3HT:PCBM blends by using (CB), (DCB), (CF), (CB:DCB), (CB:CF), and (DCB:CF) as solvents were studied using the atomic force microscopy (AFM) technique.

Figure (4) shows the surface morphologies measured using AFM for the P3HT:PCBM Bulk heterojunctions prepared from the various solvents. The root-mean- square (R.M.S) for the Bulk heterojunctions dissolved with the various solvents such as the (**a**) CB, (**b**) DCB, (**c**) CF solvents and the (**d**) CB:DCB, (**e**) CB:CF, and (**f**) DCB:CF co-solvents, were found to be 3.62, 3.89, 4.13, 4.32, 6.63, and 6.88 nm, respectively. These results indicate that the P3HT:PCBM bulk heterojunction prepared from the DCB:CF nm co-solvent has a coarser film surface morphology compared to the samples since it shows a higher R_{max} value of 6.88 nm. This rough film surface results in a large surface area and so leads to an improved efficiency in the charge generation through the effective incidence of the photons. The rough film surface is probably the signature of a polymer self-organization, which in turn enhances the ordered structure formation found in the thin film [18]. This ordered structure reduces the internal series resistance of the device, thus increasing the photocurrent [18]. It may be noted that the evaporation rates and the solubility of the solvents can affect the surface morphologies of the polymer bulk heterojunctions. By mixing both solvents together, the evaporation rate of the co-solvent is modified, resulting in different surface morphologies. In addition, the solvating activation energy also significantly influences the morphology of the films, because a good solvent may produce a better extension of the polymer chain in a solid state thin film.

Considering the results of the surface morphologies as they are affected by the various solvents, a high vapor density, a low solubility, and the evaporation rate in the CB solvent, as shown in Table (1), lead to a rough film surface when they are spin coated on the PEDOT:PSS:AuNPS/P3HT:PCBM film and post-annealed at 125 $^{\circ}$C. Figure (5) shows the external quantum efficiency values of P3HT:PCBM bulk heterojunctions prepared from different solvents, such as the (CB), (DCB), (CF), solvents and the (CB:DCB), (CB:CF), and (DCB:CF) co-solvents. It was observed that the P3HT:PCBM bulk heterojunction prepared from the CB:CF co-solvent showed the highest peak external quantum efficiency value in the wavelength range from ~ 420 to 600 nm. From this result, we conjecture that the external quantum efficiency values may be related to the absorption results show that the CB:CF blend layer absorb significantly stronger than that of all solvents [19]. The highest peak of external quantum efficiency value can be attributed to the crystalline property as well as the surface morphology of P3HT:PCBM bulk heterojunction.

Figure (6) shows the current density versus voltage (*J-V*) characteristic curves and device parameters of the parameters short-circuit current density (J_{sc}), open-circuit voltage (V_{oc}), fill factor (*FF*) and power conversion efficiency (*PCE*) values of the organic solar cells with P3HT:PCBM bulk heterojunctions prepared from the various solvents. The parameter values for the PEDOT:PSS:AuNPs/P3HT:PCBM film dissolved with the various solvents such as the (a) CB, (b) DCB, (c) CF solvents and the (d) CB:DCB, (e) CB:CF, and (f) CB:DCB, co-solvents.

The maximum parameters J_{sc}, V_{oc}, and *FF* values were found to be 8.5 mA/cm^2, 0.67 mV and 0.63, respectively for the PEDOT:PSS:AuNPs/P3HT:PCBM film using the CB:CF co-solvent, indicating that the *PCE* calculated to 3.6. From our experiments, it may be concluded that the observed improvement in the electrical

properties of the organic solar cells with the PEDOT:PSS:AuNPs/P3HT:PCBM film dissolved with the CB:CF co-solvent is caused by a favorable change in the enhanced crystallinity, the absorption light intensity, and the rough surface morphology of the bulk heterojunction due to the high vapor density and low solubility of the mixing solvents [20]. The J_{sc}, V_{oc}, and *FF* values of the organic solar cells with P3HT:PCBM bulk heterojunctions prepared from the various solvents such as pure and co-solvents are summarized in Table 2.

CONCLUSION

Organic solar cell devices with different solvents, such as (CB), (DCB), (CF), and co-solvent (CB:DCB), (CB:CF), and (DCB:CF) were fabricated. We have investigated the effect of different solvents on the crystallization and interchain of P3HT, PCBM and gold nanoparticles in PEDOT:PSS as buffer layer films using UV–vis, XRD, PL, and Raman spectroscopy. The device fabricated from CB:CF co-solvent show the improved performances of PCE 3.6%. The different solubility and evaporation rate of the mixed solvent influence the morphological structure which brings the improved performance to increase photocurrent and fill factor.
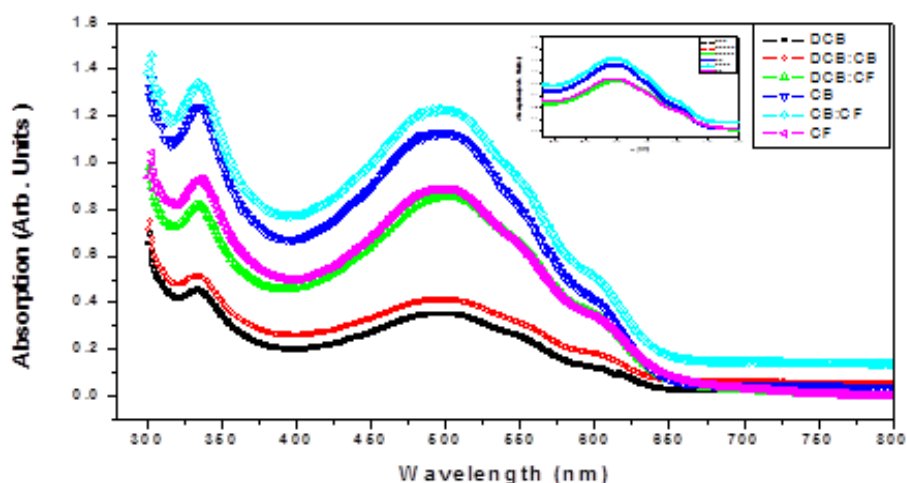
Figure (1)UV–vis absorption spectra for PEDOT:PSS:AuNPs/P3HT: PCBM films with different solvents(CB), (DCB), (CF), (CB:DCB), (CB:CF), and (DCB:CF).
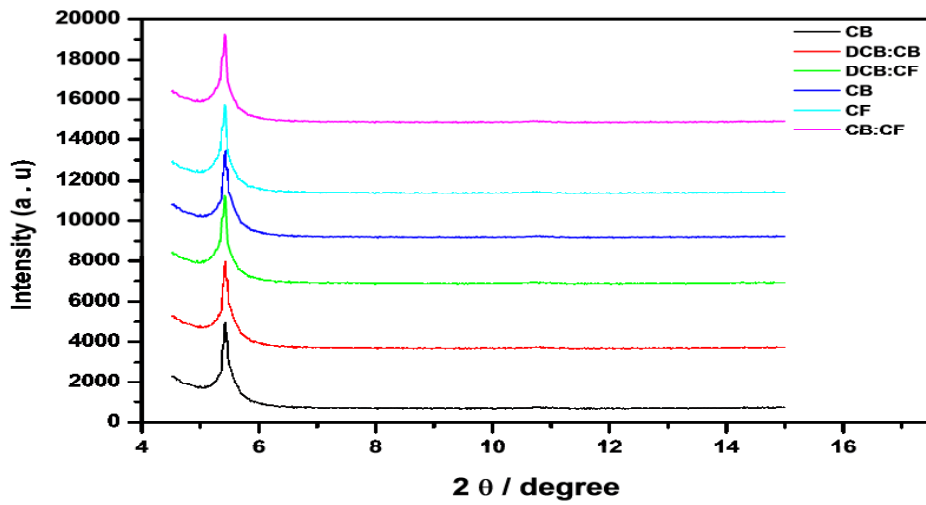
Figure (2) XRD curves for PEDOT:PSS:AuNPs/P3HT:PCBM films with different solvents (CB), (DCB), (CF), (CB:DCB), (CB:CF), and (DCB:CF).
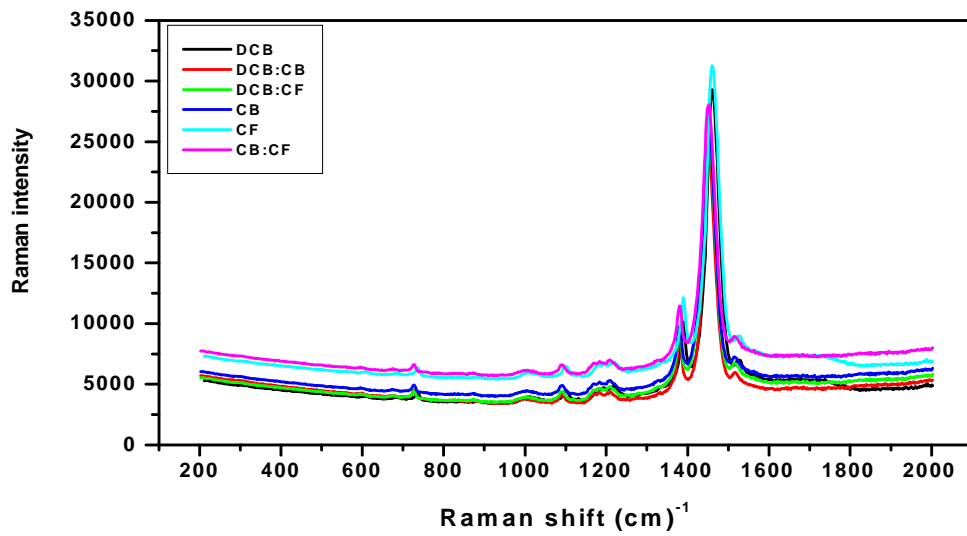
Figure (3) Raman spectroscopy of PEDOT:PSS:AuNPs/P3HT:PCBM films with different solvents (CB),(DCB),(CF),(CB:DCB),(CB:CF), and (DCB:CF).
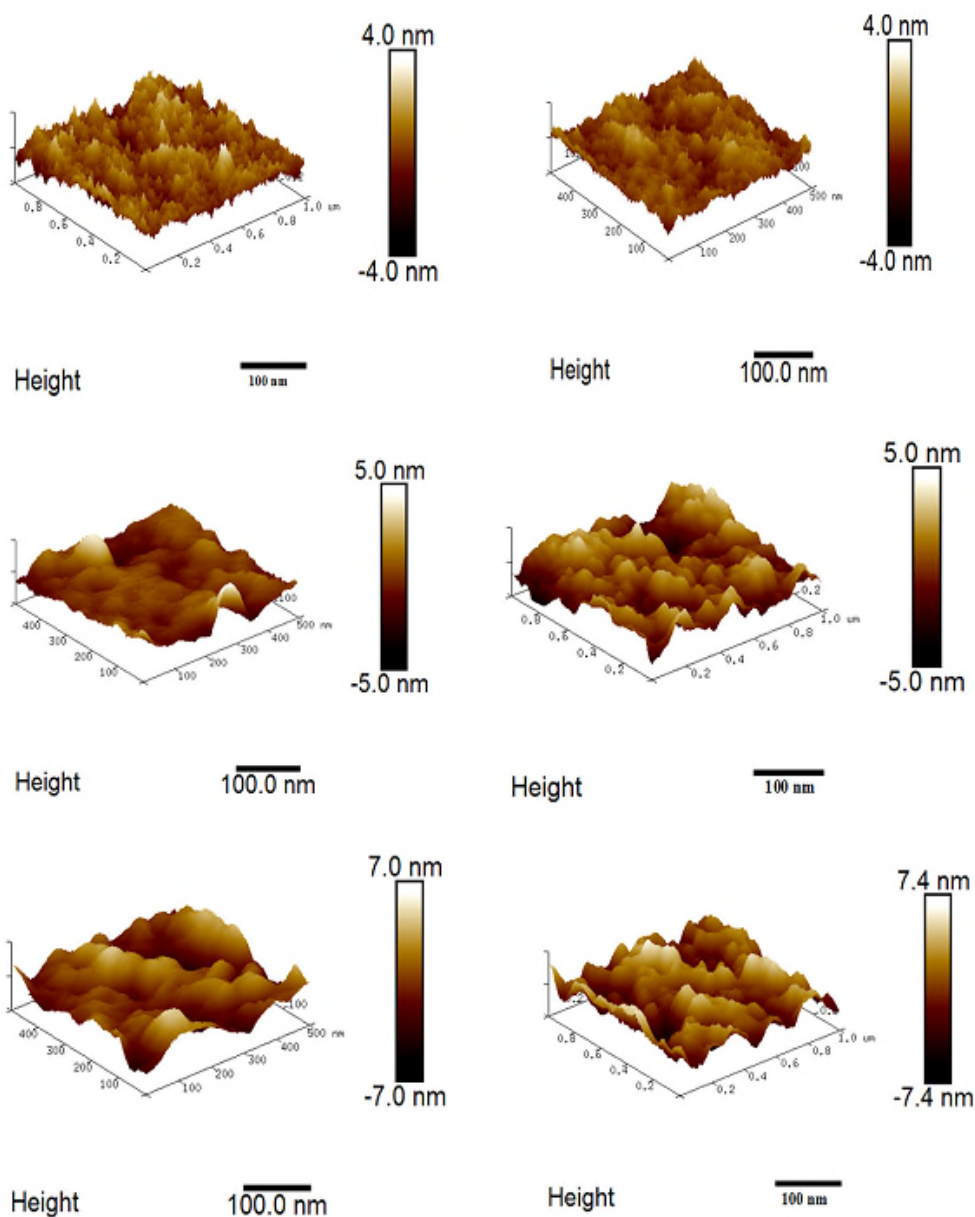
Figure(4) AFM images of PEDOT:PSS:AuNPs/P3HT:PCBM films with different solvents (CB), (DCB), (CF), (CB:DCB), (CB:CF), and (DCB:CF).
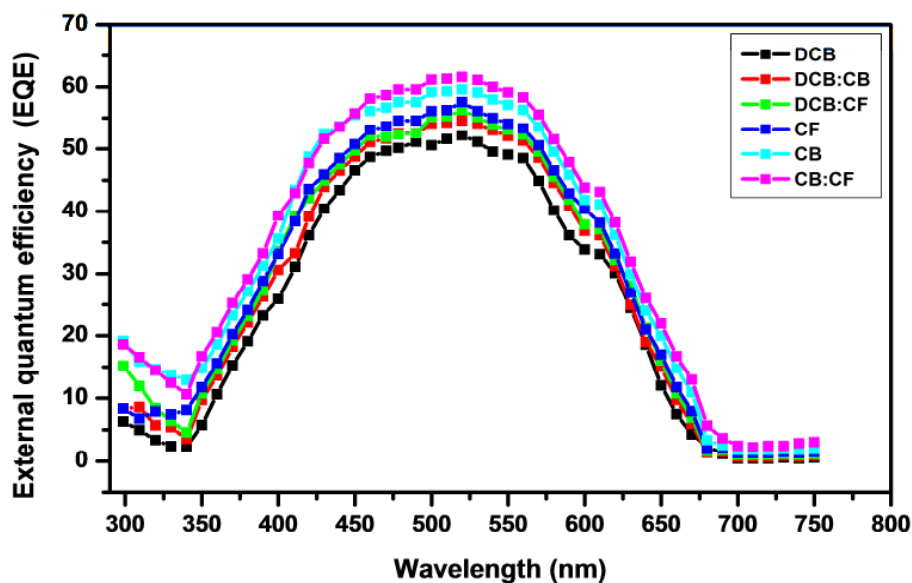
**Figure (5) External quantum efficiency spectra of PEDO:PSS:
AuNPs/P3HT:PCBM films with different solvents (CB), (DCB), (CF),
(CB:DCB), (DCB:CF), and (CB:CF).**
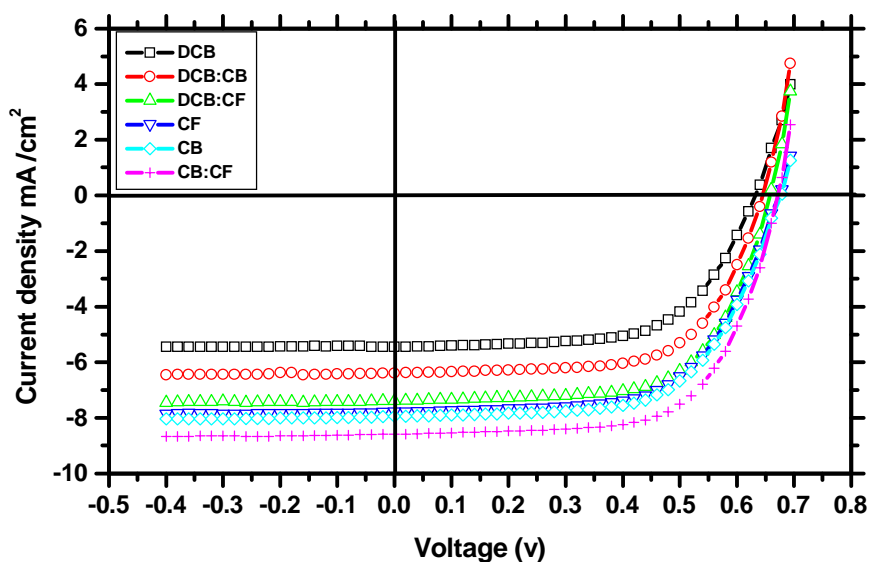
**Figure (6) J–V curves for PEDOT:PSS:AuNPs/P3HT:PCBM films with different
solvents (CB), (DCB), (CF), co- solvents (CB:DCB), (DCB:CF), and (CB:CF).**

**Table (1) AFM value for Photovoltaic properties of PEDOT:PSS:AuNPs/
P3HT:PCBM Bulk heterojunction by (CB), (DCB),(CF),(CB:DCB), (CB:CF),
and (DCB:CF).`**

solvent	R.M.S (nm)	R_a(nm)	R_{max}(nm)
DCB	3.62	3.14	18.3
CB:DCB	3.89	3.34	22.2
DCB:CF	4.13	4.03	37.2
CF	4.32	4.15	38.5
CB	6.63	6.04	49.9
CB:CF	6.88	6.34	53.9

**Table (2) Photovoltaic parameters of the organic solar cell devices with different
solvents (CB), (DCB), (CF), co- solvents (CB:DCB), (DCB:CF), and (CB:CF).**

Devices	V_{oc} (v)	J_{sc} (mA/ cm^2)	FF	PCE (%)	R_s (Ω cm^{-2})	R_{sh} (Ω cm^{-2})
DCB	0.62	5.3	0.62	2.06	10.33	926
DCB:CB	0.64	6.3	0.62	2.55	11.17	983
DCB:CF	0.65	7.3	0.60	2.9	13.64	821
CF	0.67	7.6	0.60	3	14.61	985
CB	0.67	7.8	0.61	3.2	14.52	720
CB:CF	0.67	8.5	0.63	3.6	9.98	981

REFERENCES
[1] D. Chirvase, Z. Chiguvare, M. Knipper, J. Parisi, V. Dyakonov, J.C. Hummelen, Electrical and Optical design and characterisation of regioregular poly(3-hexylthiophene-2,5diyl)/ fullerene-based heterojunction polymer solar cells, Synthetic Metals 138, 299–304, (2003).
[2] El. Jeffries, M., and R. D. McCullough, , Conjugated polymers theory, synthesis, properties, and characterization, in regioregular polythiophenes, T.A.S.a.J.R. Reynolds, Editor., CRC Press, Taylor & Francis Group, (2007).
[3] Reyes, M., Kim, K., and Carroll, D., High-efficiency photovoltaic devices based on annealed   poly(3-hexylthiophene) and 1-(3-methoxycarbonyl)-propyl-1- phenyl-(6,6) C61 blends. Applied Physics Letters, 2005. 87(083506).
[4] T. A. Chen, X. Wu, R.B. Rieke, Regio controlled Synthesis of Poly(3-alkylthiophenes) Mediated by Rieke Zinc: Their Characterization and Solid-State Properties, J. Am. Chem. Soc. 117 233, (1995).
 [6] C. J. Keavney and M. B. Spitzer, Indium-Phosphide Solar-Cells Made By Ion-Implantation, Applied Physics Letters 52 (17), 1439-1440 (1988).
[7] D. E. Carlson and C. R. Wronski, Amorphous silicon solar cell, Applied Physics Letters 28 (11), 671-673, (1976).
[8] Y. Ohtake, K. Kushiya, M. Ichikawa, A. Yamada and M. Konagai, Polycrystalline Cu(InGa)Se-2 thin-film solar cells with ZnSe buffer layers, Japanese Journal of Applied Physics Part 1-Regular Papers Short Notes & Review Papers 34 (11), 5949-5955, (1995).

[9] V. Shrotriya, J. Ouyang, and R. Tseng, Absorption spectra modification in poly(3-hexylthiophene):methanofullerene blend thin films, Chemical Physics Letters 411, 138–143, (2005).

[10] O. Ourida and B. Mohammed, Influence of the Blend Concentration of P3HT in the Performances of BHJ Solar Cells, Science Academy Transactions on Renewable Energy Systems Engineering and Technology (SATRESET), 1, 3, (2011).

[11] U. Zhokhavets, T. Erb, H. Hoppe, G. Gobsch, and S. Sariciftci N , Effect of annealing of poly(3-hexylthiophene)/fullerene bulk hetero -junction composites on structural and optical properties ,Thin Solid Films 496(2):679–682, (2006).

[12] G. Li, V. Shrotriya, Y. Yao, J. Huang, and Y. Yang, Manipulating regioregular poly(3-hexylthiophene): [6]-phenyl-C61-butyric acid methyl ester blends-route towards high efficiency polymer solar cells, J Mater Chem 17(30):3126–3140, (2007).

[13] H. Shen, P. Bienstman, and B. Maes, Plasmonic absorption enhancement in organic solar cells with thin active layers, J Appl Phys 106(7):073109, (2009).

[14] H. Sirringhaus, P. J. Brown, R. H. Friend, M. M. Nielsen, K. Bechgaard, B. M. W. Langeveld-Voss, A. J. H. Spiering, R. A. J. Janssen, E. W. Meijer, P. Herwig and D. M. de Leeuw, Two-dimensional charge transport in self-organized, high-mobility conjugated polymers, Nature, 401, 685-688 (1999).

[15] B. Grevin, P. Rannou, R. Payerne, and A. Pron, J.P. Travers, Multi-scale scanning tunneling microscopy imaging of self-organized regioregular poly (3-hexylthiophene) films, J. Chem. Phys. 118, 7097, (2003).

[16] G. LI, V. Shrotriya, J. Huangi, Y. Yao, T. Moriarty O, K. Emery, and Y. Yang, High-efficiency solution processable polymer photovoltaic cells by self-organization of polymer blends, nature materials, 4, (2005).

 [17] M. Al-lbrahim, and O. Ambacher, Effects of solvent and annealing on the improved performance of solar cells based on poly (3-hexylthiophene): fullerene, Appl. Phys. Lett. 86, 201120, (2005).

[18] B. Kippelen, and J.L. Bredas, Organic photovoltaics, Energy Environ. Sci., 2, 251, (2009).

[19] M. Grätzel, Photoelectrochemical cells, Nature, 414, 338, (2001).

[20] Y. Gao, and J. K. Gery, J. Am. Chem. Soc., Resonance Chemical Imaging of Polythiophene/Fullerene Photovoltaic Thin Films: Mapping Morphology-Dependent Aggregated and Unaggregated C=C Species, J. Am Chem Soc. 131, 9654–9662, (2009).